# Determining the structural phase transition point from the temperature of $^{40}Ca^{+}$ Coulomb crystal*

Chen Ting(陈 婷)[a)b)c)], Du Li-Jun(杜丽军)[a)b)c)], Song Hong-Fang(宋红芳)[a)b)c)], Liu Pei-Liang(刘培亮)[a)b)c)], Huang Yao(黄 垚)[a)b)], Tong Xin(童 昕)[a)b)], Guan Hua(管 桦)[a)b)†], and Gao Ke-Lin(高克林)[a)b)]

[a)] *State Key Laboratory of Magnetic Resonance and Atomic and Molecular Physics, Wuhan Institute of Physics and Mathematics, Chinese Academy of Sciences, Wuhan* 430071, *China*

[b)] *Key Laboratory of Atomic Frequency Standards, Wuhan Institute of Physics and Mathematics, Chinese Academy of Sciences, Wuhan* 430071, *China*

[c)] *University of Chinese Academy of Sciences, Beijing* 100049, *China*

(Received 25 June 2014; revised manuscript received 10 September 2014; published online 10 October 2014)

We observed the linear-to-zigzag structural phase transition of a $^{40}Ca^{+}$ crystal in a homemade linear Paul trap. The values of the total temperature of the ion crystals during the phase transition are derived using the molecular-dynamics (MD) simulation method. A series of simulations revealed that the ratio of the radial to axial secular frequencies has a dependence on the total temperature that obeys different functional forms for linear and zigzag structures, and the transition point occurs where these functions intersect; thus, the critical value of the ratio of secular frequencies that drives the structure phase transition can be derived.

**Keywords:** phase transition point, ion crystal structure, molecular-dynamics simulation

**PACS:** 37.10.Ty, 37.10.Rs, 64.70.kp **DOI:** 10.1088/1674-1056/23/12/123702

## 1. Introduction

Since Diedrich[1] and Wineland[2] successfully trapped ions in Paul traps, ion Coulomb crystals have been widely studied[3–7] because of their potential applications to quantum information processing, precise measurements, and tests of fundamental physics in a variety of fields. A ground-state-cooled linear chain of trapped ions has been experimentally demonstrated as a quantum information processor,[8–10] while a planar Coulomb crystal was shown to be a potential candidate for implementing large-scale quantum simulation and computation.[11] In particular, a cigar-shaped Coulomb crystal can be used to sympathetically cool the ions that cannot be efficiently laser-cooled directly,[12–15] which is a feature of special interest in the field of precise spectroscopy. It is important to study the structural phase transition point since applications of the ion crystal are usually structure-dependent. The transition point from a linear to a zigzag structure is crucial to studying the topological defect formation in ion crystals and testing the Kibble–Zurek scaling law.[16,17]

The ratio of the radial to axial secular frequencies is a key feature in the phase transition from a linear to a zigzag structure.[18] A linear structure is numerically predicted when the following condition is satisfied,

$$\frac{\omega_r}{\omega_z} > 0.73N^{0.86}, \tag{1}$$

where $N$ is the number of the ions and where $\omega_r$ and $\omega_z$ are the radial and axial secular frequencies respectively. A zigzag structure is expected to appear when the ratio $\omega_r/\omega_z$ drops below the critical value of $0.73N^{0.86}$.[19]

In this paper, we report both experimental and simulated results on the structural phase transition of $^{40}Ca^{+}$. The ion trap system is introduced in Section 2. The third section describes acquisition of the structural phase transition point by analyzing the total temperature of the crystal. In that section, by comparing them with experimental images, the results of a molecular dynamics (MD) simulation are used to estimate the temperatures of the Coulomb crystals. By analyzing the ion-crystal temperature, the value of the structural phase transition point is obtained.

## 2. Experimental setup

The energy levels of $^{40}Ca^{+}$ for laser cooling are shown in Fig. 1. A 397-nm diode laser is used to cool the $^{40}Ca^{+}$ ions, with the laser frequency set to a red detuning of $\Delta\omega$. An 866-nm laser is employed to re-pump the ions to the $4^2P_{1/2}$ state

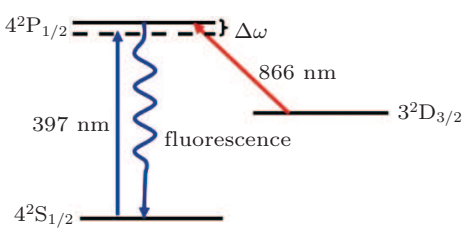



**Fig. 1.** (color online) Energy level diagram of the lowest relevant energy levels for the laser cooling of $^{40}Ca^{+}$ (not to scale).

*Project supported by the National Basic Research Program of China (Grant Nos. 2010CB832803 and 2012CB821301), the National Natural Science Foundation of China (Grant Nos. 11004222 and 91121016), and the Chinese Academy of Sciences.

†Corresponding author. E-mail: guanhua@wipm.ac.cn

© 2014 Chinese Physical Society and IOP Publishing Ltd 

because there is a certain probability that the ions decay from the $4^2P_{1/2}$ state to the $3^2D_{3/2}$ state, which has a long lifetime (1.2 s). Thus the Doppler cooling[20–22] cycle is closed.

The experimental setup is shown in Fig. 2. Calcium ions are generated by a photoionization[23] process using a 423-nm diode laser and a 375-nm LED. The background pressure is maintained at $10^{-8}$ Pa by a titanium pump. The 397-nm and 866-nm laser beams are overlapped and pass through the axis of the linear ion trap. Both of the lasers are stabilized by the transfer cavity technique[24] referred to an ultrastable 729-nm laser,[25] and the long-term drift is less than 1 MHz/hour.[26] The fluorescence of the ions is collected by a photomultiplier tube (PMT), while the image is captured by an electron-multiplying charge-coupled device (EMCCD).

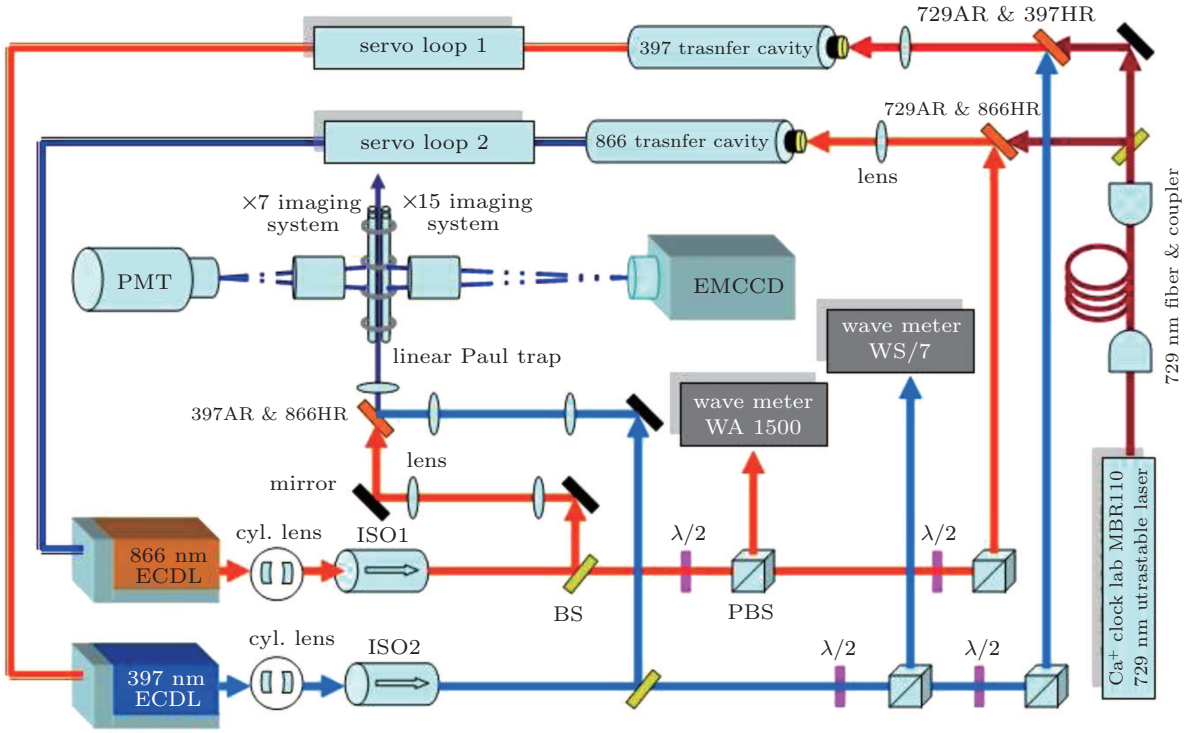



**Fig. 2.** (color online) Schematic diagram of the experimental setup.

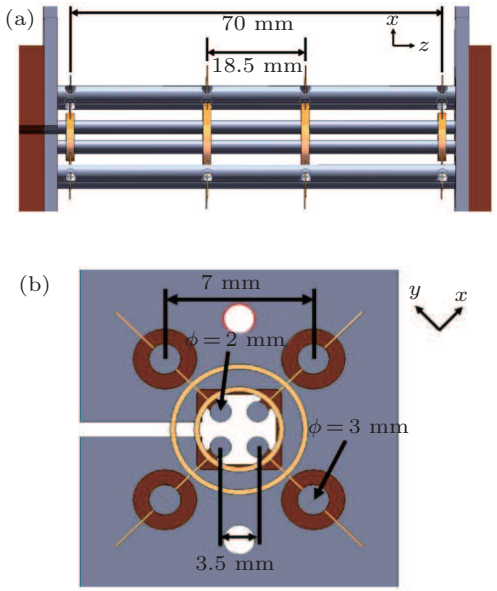



**Fig. 3.** (color online) Schematic views of the homemade linear ion trap, which is composed of four rod-shaped electrodes, four ring-shaped endcaps, and four compensating electrodes. (a) Side view of the trap. (b) Cross-sectional view of the center of the trap.

As shown in Fig. 3, the dimensions of this linear trap are similar to those of the trap used by the Hänsch group at the Max Planck Institute of Quantum Optics,[27] except for the redesigned ring-shaped endcap electrodes. There are three trapping regions, in each of which different ions can be stored. The center region is used to trap and cool calcium ions in this experiment. A dc voltage is applied to two of the inner endcaps to create axial confinement. A radio-frequency (RF) voltage $U_{\rm rf}\cos(\Omega t)$ is applied to two of the diagonally connected rods, and the other two are connected to ground. Here, $U_{\rm rf}$ is the amplitude of the radio-frequency voltage, and the RF frequency $\Omega/2\pi$ is 7.43 MHz.

## 3. Determination of the phase transition point of the Coulomb crystal

### 3.1. Experimental observation of the structural phase transition

To observe the structural phase transition, the voltage on the endcap electrodes is varied while keeping the ion numbers and other parameters the same. Figure 4 shows typical structures of the ion crystal with 22 ions in our ion trap under var-

ious conditions. The critical ratio for the structure transition to occur is calculated to be 10.42 using Eq. (1). The crystal structure corresponding to each image is determined by reading the positions of the ions in the image. A zigzag structure is confirmed when the displacement of the center ions from the axis is more than 3 pixels since the error in the ion positions can be as large as 2 pixels, while the linear ion-crystal structure consists of ions just arranged in a line. Figures 4(a1)–4(c1), which were obtained under the condition where $\omega_r/\omega_z$ was greater than the critical ratio (10.42), each shows a linear crystal structure, and figures 4(d1) and 4(e1), obtained under the condition where $\omega_r/\omega_z$ was smaller than the critical ratio (10.42), each shows a zigzag structure. The linear-to-zigzag transition occurs between Figs. 4(c1) and 4(d1). These results coincide with the predictions of Eq. (1). However, the transition point cannot be accurately determined directly from the experimental images because of the 2-pixel reading error mentioned above, which led to the ambiguity of the crystal structure near the transition point, while the MD simulations provide an accurate value for the transition point.

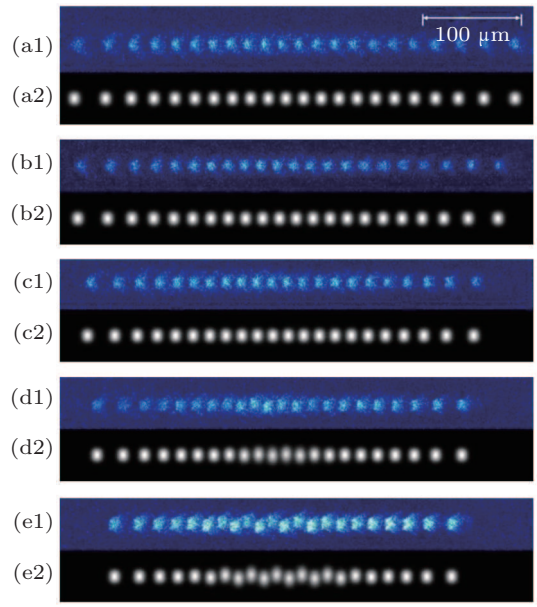



**Fig. 4.** (color online) Typical structures of an ion crystal containing 22 calcium ions. The intensity of the 397-nm laser is 74 mW/cm$^2$. The experimental images have the following properties: 4(a1) linear structure, $\omega_r/\omega_z$ = 339.5 kHz/20.6 kHz = 16.48; 4(b1) linear structure, $\omega_r/\omega_z$ = 339.5 kHz/24.4 kHz = 13.91; 4(c1) linear structure, $\omega_r/\omega_z$ = 339.5 kHz/30.4 kHz = 11.17; 4(d1) zigzag-shaped structure, $\omega_r/\omega_z$ = 339.5 kHz/33.9 kHz = 10.01; and 4(e1) zigzag-shaped structure, $\omega_r/\omega_z$ = 339.5 kHz/38.9 kHz = 8.73. The simulation images 4(a2)–4(e2) are obtained for the same parameters as the corresponding experimental images (that is 4(a1)–4(e1), respectively).

### 3.2. Determination of the phase transition point by MD simulation

The temperatures of the crystals provide much information about the crystal structures. The total temperature, which reflects both the secular motion and micromotion energies of the Coulomb crystal, strongly depends on the crystal structure when the same cooling condition is provided. When the crystal is in a loose linear structure, the excess micromotion is negligible, and the total temperature is determined mainly by secular motion and stays constant. While the linear structure gets tighter in the axial direction, the ions in the center part of the structure will extend in the radial direction and undergo excess micromotion, thus gaining more kinetic energy. When the zigzag structure is finally formed, the amplitude of the micromotion increases dramatically since most of the ions are repelled farther away from the trap axis. Therefore, the sensitivity of the total temperature to the ion structure variation provides an effective tool for obtaining the criterion for such a phase transition.

MD simulation is used to determine the temperature of the ion crystal, and the model used was described in Ref. [28]. The positions of all the ions in the simulation are projected onto the imaging plane of the EMCCD, and density plots are used to create the simulated ion crystal images. All of the simulations correspond to secular motion temperatures of 2 mK, while the total temperatures are 3.7 mK, 3.7 mK, 4.5 mK, 38.6 mK, and 111.9 mK for Figs. 4(a2)–4(e2) respectively; the total temperature is almost constant when the crystal has a linear structure, but dramatically increases when a zigzag-shaped crystal is formed. These results are in accord with the analysis presented above.

Based on this, further simulations are performed, changing the ratio of the radial and axial secular frequencies in small steps; the results are shown in Fig. 5.

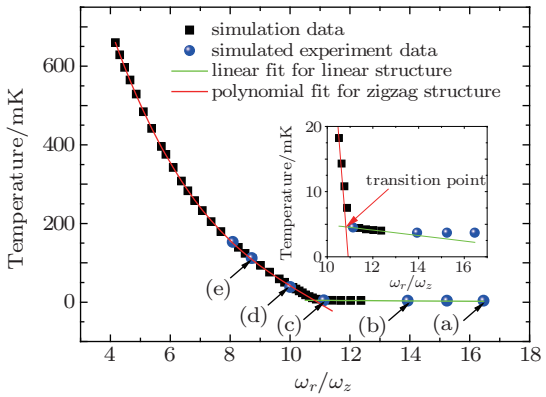



**Fig. 5.** (color online) Plot of the total temperature, showing its increasing tendency with respect to $\omega_z$, as calculated by MD simulation. The inset shows the linear structure in more detail. The blue circles represent points from the simulations that were confirmed by our experiment, and the annotations indicate the corresponding panels in Fig. 4 [(a)–(e)]; the black squares indicate the results of simulations.

Obviously, the decreasing tendency of the total temperature as the ratio $\omega_r/\omega_z$ increases can be separated into two parts, corresponding to the zigzag and linear structures respectively. Separate curve fits are made to the temperatures in the two regimes: linear fitting is used for the slowly decreasing

part, and cubic polynomial fitting is used for the rapidly decreasing part. The two fitted curves are extrapolated to a point where they intersect, at $\omega_r/\omega_z = 10.8$, which can be defined as the transition point.

However, the points between 10.63 and 11.0 cannot be fitted to either the linear or polynomial fits, since the residual errors are too large (exceeding 10%). The errors associated with those points originate from approximate calculations in the MD simulation, which lead to a region of uncertainty around the intersection point from 10.6 to 11.0, with an error of about 1.9%. This result is consistent with Eq. (1) within an error of about 3.7%.

## 4. Conclusions

In summary, $^{40}Ca^{+}$ ions have been successfully trapped and laser-cooled in our homemade linear Paul trap system. The linear-to-zigzag structural phase transition process has been studied. By analyzing the decreasing tendency of the total temperatures as the ratio $\omega_r/\omega_z$ increases, the phase transition point was obtained with an error of about 1.9%.

## Acknowledgements

We acknowledge early work on this project by Qu W and Ou B and Shi T, Yan Z, Li C, Tang L, Zhong Z, Yang W and Saathoff G for fruitful discussions.

## References

[1] Diedrich F, Peik E, Chen J M, Quint W and Walther 1987 *Phys. Rev. Lett.* **59** 2931
[2] Wineland D J, Bergquist J C, Itano W M, Bollinger J J and Manney C H 1987 *Phys. Rev. Lett.* **59** 2935
[3] Roth B, Blythe P and Schiller S 2007 *Phys. Rev. A* **75** 023402
[4] Nagerl H C, Leibfried D, Schmidt-Kaler F, Eschner J and Blatt R 1998 *Opt. Express* **3** 89
[5] Dantan A, Albert M, Marler J P, Herskind J P and Drewsen M 2009 *Phys. Rev. A* **80** 041802
[6] Bollinger J J, Mitchell T B, Huang X P, Itano W M, Tan J N, Jelenkovic B M and Wineland D J 2000 *Phys. Plasmas* **7** 7
[7] Asprusten M, Worthington S and Thompson R C 2014 *Appl. Phys. B* **114** 157
[8] Leibfried D, Knill E, Seidelin S, Britton J, Blakestad R B, Chiaverini J, Hume D B, Itano W M, Jost J D, Langer C, Ozeri R, Reichle R and Wineland D J 2005 *Nature* **438** 639
[9] Kim K, Chang M S, Korenblit S, Islam R, Edwards E E, Freericks J K, Lin G D, Duan L M and Monroe C 2010 *Nature* **465** 590
[10] Monz T, Schindler P, Barreiro J T, Chwalla M, Nigg D, Coish W A, Harlander M, Hänsel W, Hennrich M and Blatt R 2011 *Phys. Rev. Lett.* **106** 130506
[11] Porras D and Cirac J I 2006 *Phys. Rev. Lett.* **96** 250501
[12] Roth B, Fröhlich U and Schiller S 2005 *Phys. Rev. Lett.* **94** 053001
[13] Barletta P, Tennyson J and Barker P F 2009 *New J. Phys.* **11** 055029
[14] Soldán P and Huston J 2004 *Phys. Rev. Lett.* **92** 163202
[15] Tong X, Winney A H and Willitsch S 2010 *Phys. Rev. Lett.* **105** 143001
[16] Ulm S, Rossnagel J, Jacob G, Degunther C, Dawkins S T, Poschinger U G, Nigmatullin R, Tetzker A, Plenio M B, Schmidt-Kaler F and Singer K 2013 *Nat. Commun.* **4** 2290
[17] Pyka K, Keller J, Partner H L, Nigmatullin R, Burgermeister T, Meier D M, Kuhlmann K, Retzker A, Plenio M B, Zurek W H, del Campo A and Mehlstaubler T E 2013 *Nat. Commun.* **4** 2291
[18] Block M, Drakoudis A, Leuthner H, Seibert P and Werth G 2000 *J. Phys. B: At. Mol. Opt. Phys.* **33** 375
[19] Steane A 1997 *Appl. Phys. B* **64** 623
[20] Wineland D J, Drullinger R E and Walls F L 1978 *Phys. Rev. Lett.* **40** 1639
[21] Neuhauser W, Hohenstatt M, Toschek P and Dehmelt H 1978 *Phys. Rev. Lett.* **41** 233
[22] Hänsch T W and Schawlow A L 1975 *Opt. Commun.* **13** 68
[23] Gulde S, Rotter D, Barton P, Schmidt-Kaler F, Blatt R and Hogervorst W 2011 *Appl. Phys. B* **73** 861
[24] Chwalla M, Benhelm J, Kim K, Kirchmair G, Monz T, Riebe M, Schindler P, Villar A S, Hänsel W, Roos C F, Blatt R, Abgrall M, Santarelli G, Rovera G D and Laurent Ph 2009 *Phys. Rev. Lett.* **102** 023002
[25] Huang Y, Liu Q, Cao J, Ou B Q, Liu P, Guan H, Huang X and Gao K 2011 *Phys. Rev. A* **84** 053841
[26] Qu W, Huang Y, Guan H, Huang X and Gao K 2011 *Chin. J. Lasers* **38** 0802008
[27] Semczuk M 2009 "An Ion Trap for Laser Spectroscopy on Lithium Ions" (MS thesis) (Warsaw: University of Warsaw and Max Planck Institute of Quantum Optics) (in Germany)
[28] Zhang C, Offenberg D, Roth B, Wilson M A and Schiller S 2007 *Phys. Rev. A* **76** 012719